Contents lists available at ScienceDirect

Journal of Contaminant Hydrology

journal homepage: www.elsevier.com/locate/jconhyd

An explanation for differences in the process of colloid adsorption in batch and column studies

Svantje Treumann [a], Saeed Torkzaban [a,*], Scott A. Bradford [b], Rahul M. Visalakshan [a], Declan Page [a]

[a] CSIRO Land and Water, Glen Osmond, SA 5064, Australia
[b] USDA, ARS, Salinity Laboratory, Riverside, CA 92507, United States

ARTICLE INFO

Article history:
Received 16 April 2014
Received in revised form 5 June 2014
Accepted 13 June 2014
Available online 20 June 2014

Keywords:
Colloid
Bacteria
Batch
PARP-1
Column experiments
Porous media
Attachment

ABSTRACT

It is essential to understand the mechanisms that control virus and bacteria removal in the subsurface environment to assess the risk of groundwater contamination with fecal microorganisms. This study was conducted to explicitly provide a critical and systematic comparison between batch and column experiments. The aim was to investigate the underlying factors causing the commonly observed discrepancies in colloid adsorption process in column and batch systems. We examined the colloid adsorption behavior of four different sizes of carboxylate-modified latex (CML) microspheres, as surrogates for viruses and bacteria, on quartz sand in batch and column experiments over a wide range of solution ionic strengths (IS). Our results show that adsorption of colloids in batch systems should be considered as an irreversible attachment because the attachment/detachment model was found to be inadequate in describing the batch results. An irreversible attachment-blocking model was found to accurately describe the results of both batch and column experiments. The rate of attachment was found to depend highly on colloid size, solution IS and the fraction of the sand surface area favorable for attachment (S_f). The rate of attachment and S_f values were different in batch and column experiments due to differences in the hydrodynamic of the system, and the role of surface roughness and pore structure on colloid attachment. Results from column and batch experiments were generally not comparable, especially for larger colloids ($\geq$0.5 μm). Predictions based on classical DLVO theory were found to inadequately describe interaction energies between colloids and sand surfaces.

1. Introduction

An understanding and ability to predict the transport and fate of colloids such as viruses, bacteria, protozoa, clay minerals, and engineered nanoparticles in porous media is essential for a wide variety of environmental and engineering applications (Bradford et al., 2012; Mondal and Sleep, 2013; Schijven and Hassanizadeh, 2000; Torkzaban et al., 2013). Colloid transport and fate are strongly influenced by retention in porous media (Ryan and Elimelech, 1996; Shen et al., 2008). Extensive theoretical and experimental studies have therefore been devoted to understanding and quantifying colloid retention in porous media (reviews are given by Bradford et al., 2014; Ginn et al., 2002; Harvey et al., 2002; Jin and Flury, 2002). It has been shown that colloid retention depends on a range of physicochemical and hydrodynamic conditions (Li and Johnson, 2005; Li et al., 2004; Pensini et al., 2012; Torkzaban et al., 2008; Tufenkji and Elimelech, 2004). Batch and column experiments are the most common methods to study colloid retention in saturated porous media. These experimental techniques offer the advantage that retention can be examined under well-defined conditions. However, numerous discrepancies between batch and column results have been reported in the literature (e.g. Bales et al., 1991; Sadeghi et al., 2013; Zhao et al., 2008).

* Corresponding author. Tel.: +61 8830 38491.
E-mail address: Saeed.Torkzaban@csiro.au (S. Torkzaban).

http://dx.doi.org/10.1016/j.jconhyd.2014.06.007
0169-7722/

Packed-column experiments are commonly utilized to study colloid transport and retention processes over a range of physical and chemical conditions. Analysis of colloid breakthrough curves (BTCs), and sometimes retention profiles (RPs) following completion of the experiment, are used to determine values of attachment and detachment rate constants (Harvey and Garabedian, 1991; Johnson et al., 2007; Schijven et al., 2000; Tong et al., 2005). These retention parameters are determined by fitting the solution of a mass balance transport model to experimental BTCs and/or RPs (Kim et al., 2009). The bulk of existing literature from column studies considers colloid transport to be controlled by attachment and detachment processes (Bradford et al., 2014; Schijven et al., 2000). These studies have demonstrated that the diffusion-controlled detachment rate is very slow during steady-state flow and chemical conditions (Ryan and Elimelech, 1996; Torkzaban et al., 2013). In addition to attachment, colloid straining (retention in grain–grain contacts and surface roughness) may also play a significant role in colloid retention (Bradford et al., 2013; Ma et al., 2011). However, determination of the relative contribution of attachment and straining to retention is difficult, if not impossible, from only BTC and RP information (Bradford et al., 2009). Microscopic observations have been employed to identify specific mechanisms of colloid retention, but quantitative determination of the relative contributions of these mechanisms is still not possible. Moreover, recent studies have pointed out that colloid retention in packed-bed columns is limited to only a small fraction of the solid surfaces, and blocking-type behavior is typically observed if the input colloid concentration is high and/or the colloid injection continues for a relatively long time (Brown and Abramson, 2006).

Batch experiments are carried out by adding a quantity of solid (e.g. sand) into a solution containing a known concentration of colloids. The mixture is subsequently shaken for a sufficient period of time to reach a steady-state (equilibrium) condition. The final concentration of colloids in solution is measured and the amount of attached colloids is calculated from mass balance calculations. The apparent steady-state concentrations are used to construct equilibrium isotherms using linear, Langmuir, or Freundlich models (Yates et al., 1987). The attachment process is typically considered to be linear and reversible (Schijven and Hassanizadeh, 2000). In this case, a distribution coefficient (K_D) is calculated and converted to a retardation factor (R) that may be used in transport studies. Colloid attachment and detachment rate coefficients can also be determined from batch studies provided that the colloid concentration in the aqueous phase is measured at various times before the steady-state concentration is reached (Sadeghi et al., 2013). However, attachment and detachment rates from batch experiments have not always been consistent and reproducible due to some yet-unknown factors (Chrysikopoulos and Aravantinou, 2012; Sadeghi et al., 2013; Syngouna and Chrysikopoulos, 2010; Thompson and Yates, 1999; Thompson et al., 1998; Zhao et al., 2008). Such factors may include the type and size of the container, the presence or absence of the air–water interface in the system, the method of shaking to achieve complete mixing, and the ratio of solid and liquid phases in the container.

A potential advantage of batch experiments is that they involve less space and labor than column studies. However, results of batch studies have not been consistent with those of column or field experiments (Sadeghi et al., 2013; Schijven and Hassanizadeh, 2000). Column experiments usually show no retardation in the BTCs, suggesting that a kinetic attachment process should be considered and that the rates of attachment and detachment are slow (Bales et al., 1991; Johnson and Elimelech, 1995; Kim et al., 2009). Batch experiments have been found to either overestimate (Sadeghi et al., 2013; Schijven et al., 2000; Zhao et al., 2008) or underestimate colloid attachment compared with that observed in column studies (Schijven et al., 2000; Torkzaban et al., 2008). This discrepancy has been attributed to the time duration of batch experiments and the selected solid/solution ratios (Sadeghi et al., 2013). Alternatively, differences in batch and column experiments may also be related to the hydrodynamic conditions, surface roughness, and pore structure. In particular, the solid phase is continuously mixed and the flow direction changes during batch experiments. This facilitates the collision of colloids to the solid phase, and possibly higher attachment rates, but also eliminates the pore structure and continuously changes the applied hydrodynamic (T_H) and resisting adhesive (T_A) torques that act on the colloids retained at roughness locations on the solid phase. Conversely, the solid phase in column experiments is stationary, and the colloids retained at surface roughness locations and grain–grain contacts will always experience a lower applied hydrodynamic torque and greater resisting adhesive torque (Bergendahl and Grasso, 2000; Bradford et al., 2009; Ma et al., 2011; Torkzaban et al., 2010a). The solid surface area associated with colloid retention is therefore expected to be greater in column than batch systems. Furthermore, the potential influence of blocking on the kinetic of colloid attachment has not been investigated in batch studies.

This study has been explicitly designed to provide a critical and systematic comparison between batch and column experiments. The aim was to investigate the underlying factors causing the commonly observed discrepancies in colloid adsorption in column and batch experiments. We examined the adsorption behavior of four different sizes of carboxylate-modified latex (CML) microspheres in batch and column experiments. The advantage of using CML microspheres is that the influence of confounding factors on retention data can be minimized; e.g., particle aggregation for engineered nanoparticles, and inactivation and growth for microbes. Our results show that colloid adsorption in batch systems should be considered as an irreversible attachment process with a blocking behavior. The rate of attachment and the fraction of the surface area contributing to colloid immobilization (S_f) were much smaller in batch than column experiments due to differences in the hydrodynamics, and the role of surface roughness and pore structure. Results from column and batch experiments were generally not comparable, especially for larger colloids ($\geq$0.5 μm). We believe this study is the first to systematically compare differences in colloid retention in batch and column studies.

2. Material and methods

2.1. Colloids, sand, and electrolyte solutions

Ultra pure quartz sand (Charles B. Chrystal Co., Inc., NY) was employed as the porous media for the column and batch experiments. The median grain diameter of the sand

was 250 μm, and the coefficient of uniformity was 1.4 ($U = d_{60}/d_{10}$), where x% of the mass is finer than d_x. Prior to use the quartz was cleaned thoroughly to remove impurities. The cleaning steps included soaking the sand in 37% HCl (Fisher) for 24 h, washing in deionized water and drying at 105 °C.

Various electrolyte solutions were made using Milli-Q water as the aqueous solution. The pH was unbuffered and ranged from 5.6 to 5.8. The solution IS was adjusted by adding NaCl to achieve IS ranging from 0 to 800 mM (Merck Pty Ltd., Product 10241J, AnalaR).

Fluoresbrite®Yellow-Green CML microspheres (Polysciences, Inc.) were used as model colloids in batch and column experiments due to their spherical shape, well-defined size and surface charge, and ease in detection at low concentration. Four sizes (2, 1, 0.5 and 0.1 μm) of CML microspheres were used in batch experiments, whereas only three sizes (2, 0.5 and 0.1 μm) were employed in column experiments. The colloid concentration was determined using a fluorometer (Synergy MxF Monochromator-Based Fluorescence Microplate Reader, Biotec) at an excitation wavelength of 441 nm and an emission wavelength of 486 nm. Stock suspensions from the manufacturer were diluted in selected electrolyte solutions to achieve an initial concentration (C_0) for batch experiments of 1.4×10^6, 1.1×10^7, 9.1×10^7, and 2.8×10^{10} N_c mL^{-1} for the 2, 1, 0.5, and 0.1 μm colloids, respectively. Several batch experiments with the 0.1 and 0.5 μm colloids were also conducted at a higher initial concentration of 2.0×10^8 and 9.1×10^8 N_c mL^{-1} for the 0.5 μm and 6.3×10^{10} and 2.8×10^{11} N_c mL^{-1} for the 0.1 μm colloids. For the column experiment influent concentrations of 1.1×10^6, 7.3×10^7 and 2.3×10^{10} N_c mL^{-1} for the 2, 0.5 and 0.1 μm colloids, respectively were used.

2.2. Electrokinetic characterization and DLVO calculations

The electrophoretic mobility of the colloids and crushed sand grains was measured in various NaCl electrolyte solutions using a Zetasizer (Malvern, Zetasizer Nano Series, Nano-ZS). The Smoluchowski equation was used to convert the measured electrophoretic mobility values to zeta potentials. The measurements were repeated five times for each colloid suspension. Average zeta potential values are reported in Table 1. Classical DLVO theory (Derjaguin and Landau, 1941) was used to calculate the total interaction energy (the sum of London–van der Waals attraction and electrostatic double-layer repulsion) for the colloids upon close approach to quartz surfaces (assuming sphere–plate interactions) for the various IS solutions used in our experiments. Retarded London–van der Waals attractive interaction force was determined from the expression of Gregory (1981) utilizing a value of 4.04×10^{-21} J for the Hamaker constant (Bergendahl and Grasso, 1999) to represent the latex–water–quartz system. In these calculations, constant-potential electrostatic double layer interactions were quantified using the expression of Hogg et al. (1966), with zeta potentials in place of surface potentials.

2.3. Batch experiments

Batch experiments were conducted to determine the attachment behavior of the CML colloids to quartz sand in the absence of pore structure, where the entire system is in motion. These experiments were conducted by placing 31 g of sand and 31 mL of a known initial concentration of the colloid suspension into 42 mL glass tubes with the temperature kept at approximately 20 °C. All tubes were completely filled with the colloid suspension to eliminate any presence of air, which might influence colloidal attachment in the system (Lazouskaya and Jin, 2008; Thompson and Yates, 1999; Thompson et al., 1998). Various solution IS were considered in the batch studies, as indicated in Table 1. To provide complete mixture of the system during the experiment, the tubes were rotated on a 45° angle with a tube rotator (Scilogex, Mx-Rd-Pro LCD) at a speed of 10 rpm. The colloid concentration was determined in the batch system at time intervals of 0, 10, 20, 30, 60, 120 and 180 min (total of 3 h). Following the completion of the attachment phase (i.e., 3 h of continuous shaking), some of the batch tubes underwent additional experimental phase to examine the reversibility of colloid attachment in the batch system. In this case, the colloid suspension in the batch tubes was removed and replaced with colloid-free electrolyte solution of the same chemical composition. The tubes were subsequently shaken for another 2 h, and the initial and final colloid concentration of the aqueous phase was measured.

Duplicates were carried out for all experiments to ensure repeatability. Additionally, a set of control tubes with only colloid suspension was prepared to ensure the stability of the colloids over the course of the experiments. Control tubes of sand and electrolyte solutions without colloids were also performed to measure the background colloid concentration originating from the sand. It was confirmed that the fluorometer

Table 1
The average of zeta potentials of colloids and quartz sand as well as calculated DLVO interaction parameters in the indicated solution chemistries.

D_c (μm)	IS (mM)	Zeta potential (mV)		Energy barrier (kT)	Secondary min. depth (kT)	Secondary min. separation (nm)
		Colloid	Sand			
2	1	−68	−40	4403	−0.65	149
2	10	−48	−22	1543	−3.5	35.5
2	50	−37	−15	556	−10.6	12
2	100	−21	−11	73	−20.4	6
2	300	−16	−10	ND[a]	ND	ND
2	500	−12	−9	ND	ND	ND
1	1	−65	−40	2121	−0.24	151
1	10	−59	−22	949	−1.5	37
1	50	−34	−15	245	−5.1	12
1	100	−27	−11	69	−9.2	6.5
1	300	−21	−10	ND	ND	ND
1	500	−17	−9	ND	ND	ND
0.5	1	−60	−40	993	0.08	154
0.5	10	−51	−22	411	−0.6	36.5
0.5	30	−49	−19	300	−1.5	18.5
0.5	50	−34	−15	123	−2.4	12
0.5	100	−22	−11	22	−4.6	6
0.5	300	−17	−10	ND	ND	ND
0.1	1	−58	−40	194	−0.002	178
0.1	10	−52	−22	85	−0.05	39.5
0.1	30	−43	−19	52	−0.16	19
0.1	50	−32	−15	23	−0.3	12.5
0.1	100	−19	−11	3.2	−0.7	6
0.1	300	−15	−10	ND	ND	ND

[a] Not determined.

did not detect any background colloid concentration originating from the sand over the range of tested IS.

The decrease in colloid concentration with time in the batch systems was attributed to attachment to the sand surface. The governing equations describing first-order attachment and detachment processes are given as:

$$V_w \frac{\partial C}{\partial t} = -V_w k_{att} \psi C + M_s k_{det} S \quad (1)$$

$$M_s \frac{\partial S}{\partial t} = V_w k_{att} \psi C - M_s k_{det} S \quad (2)$$

where C [$N_c\ L^{-3}$; where N_c and L denote the number of colloids and units of length, respectively] is the colloid concentration in the aqueous phase, t [T; T denotes units of time] is the time, M_s [M; M denotes units of mass] is the dry mass of sand, S [$N_c\ M^{-1}$] is the solid phase concentration of attached colloids, V_w [L^3] is the volume of water, k_{att} [T^{-1}] is the colloid attachment coefficient, k_{det} [T^{-1}] is the colloid detachment coefficient, and Ψ [−] is a dimensionless function that is used to account for a reduction in the attachment rate due to blocking (filling up) of favorable attachment sites. A Langmuirian model is used to describe Ψ as (Adamczyk et al., 1994):

$$\psi = \frac{S_{max} - S}{S_{max}} = 1 - \frac{S}{S_{max}} \quad (3)$$

where S_{max} [$N_c\ M^{-1}$] is the maximum solid phase concentration of attached colloids. Eqs. (1)–(3) were numerically solved using the COMSOL software package (COMSOL, Inc., Palo Alto, California), subject to the initial conditions ($t = 0$) of $C = C_0$ and $S = 0$. The model parameters C_0, M_s, and V_w were obtained directly from experimental measurements, whereas the values of k_{att} and S_{max} were determined by fitting of Eqs. (1)–(3) to observed batch concentration data. In all cases, the k_{det} value was set to zero as discussed later in the paper.

The fraction of the solid surface area that is available for attachment (S_f) may be determined from fitted S_{max} values using the following equation:

$$S_f = \frac{A_c \rho_b S_{max}}{(1-\gamma) A_s} \quad (4)$$

where A_c [$L^2\ N_c^{-1}$] is the cross section area per colloid, A_s [L^{-1}] is the solid surface area per unit volume, i.e. the collector surface area per unit volume of porous media, and γ [−] is the porosity of a monolayer packing of colloids on the solid surface. In this work we assume a value of $\gamma = 0.5$ in all simulations based on information presented by Johnson and Elimelech (1995).

2.4. Column experiments

The column experiments were performed using acrylic columns with a length of 11 cm and a radius of 1 cm. The columns were wet packed, where the water level was always kept above the sand surface, with ~45 g of quartz sand. The average grain diameter of the sand was 255 μm, and the grain size ranged between 106 and 300 μm. The porosity was calculated gravimetrically to be 0.4, and the volume associated with one pore volume (PV) was 13.8 cm^3. A syringe pump (Harvard Apparatus 22) was used to pump the solutions into the column at a steady rate. A fraction collector (Spectra/Chrom® CF-1 Fraction Collector) was used to continuously collect the effluent samples. The average pore water velocity was maintained at 5 m/d for all experiments. A pulse of colloid suspension was injected for three pore volumes (PV), followed by a colloid-free electrolyte solution. Colloid transport experiments were conducted in duplicate at each solution IS. Sodium nitrate ($NaNO_3$) was used as a conservative tracer to determine the pore water velocity and the dispersivity. Two pore volumes of 1 mM $NaNO_3$ were pumped into the column and the breakthrough of NO_3^- was monitored by measuring the absorbance of the effluent at 210 nm using a spectrophotometer.

The HYDRUS-1D code (Simunek et al., 2005) was used to simulate the colloid transport and retention in the columns. Relevant aspects of this code are described below. The code numerically solves the advection–dispersion equation that accounts for colloid retention in the column as given below:

$$\frac{\partial C}{\partial t} = \lambda \nu \frac{\partial^2 C}{\partial z^2} - \nu \frac{\partial C}{\partial z} - r_d \quad (5)$$

where λ [L] is the dispersivity, v [LT^{-1}] is the average pore-water velocity, and r_d [$N_c\ L^{-3}\ T^{-1}$] is the retention rate of colloids on the solid phase. The value of r_d is given by:

$$r_d = \rho_b \frac{\partial S}{\partial t} = n k_{att} \left(1 - \frac{S}{S_{max}}\right) C - \rho_b k_{det} S \quad (6)$$

where ρ_b [ML^3] is the sand bulk density and n [−] is the porosity. HYDRUS-1D is coupled to a non-linear least squares optimization routine based on the Levenberg–Marquardt algorithm (Marquardt, 1963) to fit model parameters (i.e. S_{max}, k_{att}) to breakthrough curves.

3. Results and discussion

3.1. DLVO calculations

Table 1 shows that the zeta potential of the colloids and sand became less negative as the IS increased due to compression of the electrostatic double layer thickness (Bhattacharjee et al., 1998). This data was used in DLVO calculations to estimate the total interaction energy between colloids (2, 1, 0.5 and 0.1 μm) and the quartz collectors for the various IS levels. The energy barrier heights, and depths and separation distances for the secondary minima are listed in Table 1. These DLVO calculations predict the absence of a repulsive energy barrier to colloid attachment to the sand surface and the existence of primary minimum interactions when IS ≥ 100 mM. Conversely, a substantial energy barrier is predicted to occur for all of these colloids when the IS ≤ 50 mM. The energy barriers increase with an increase in colloid size and a decrease in IS, ranging from 3.2 kT at IS = 100 mM for 0.1 μm colloids to over 4000 kT at IS = 1 mM for 2 μm colloids. These energy barriers suggest that it is unlikely for the colloids to attach in the primary energy minimum when the IS ≤ 100 mM. Furthermore, macroscale chemical heterogeneities that may produce primary minimum interactions are expected to be negligible for the ultra-pure

quartz sand. However, colloid retention in a secondary minimum is possible when the depth of the secondary minimum is greater than the thermal energy of diffusing colloids (Shen et al., 2007; Simoni et al., 1998). This occurs when the absolute magnitude of the secondary energy minimum is greater than around 1.5 kT. The depth of the secondary minimum tends to increase with colloid size and IS as shown in Table 1.

3.2. Batch experiments

Batch experiments were conducted over a wide range of solution IS in order to systematically examine the attachment and detachment behavior of the various colloid sizes (2, 1, 0.5, and 0.1 μm). Fig. 1 presents plots of the normalized colloid concentrations (C/C_0; where C_0 is the initial colloid concentration) as function of time for the various IS and colloid sizes in the batch systems. We did not observe any colloid attachment to the sand surfaces at IS = 1 or 10 mM for all colloid sizes. However, the concentration of colloids in the solution began to decrease with further increases in the IS as a result of attachment. In general, values of C/C_0 rapidly decreased with time and then eventually approached a quasi-steady state concentration level. The amount and dynamics of the colloid attachment process were strong functions of the solution IS and the colloid size; increasing with IS and decreasing with colloid size. Each of these observations will be examined in detail below.

A first-order kinetic attachment and detachment model (Eqs. (1) and (2) with $\psi = 1$) is commonly used to simulate the kinetic of colloid attachment in batch systems (Schijven and Hassanizadeh, 2000). In this case, the value of C/C_0 is assumed to approach equilibrium conditions as time increases. If colloid attachment is consistent with a linear and equilibrium adsorption process, then an equilibrium partition coefficient between colloids in the aqueous and solid phases (K_D) can be defined in terms of k_{att} and k_{det} as $K_D = \frac{V_w k_{att}}{M_s k_{det}}$ (Schijven and Hassanizadeh, 2000). The value of K_D can be related to a retardation coefficient for breakthrough concentrations (BTCs) obtained in transport studies. Alternatively, the trend of decreasing C/C_0 with time can also be explained by irreversible attachment and blocking (filling up) of available attachment sites (Eqs. (1) and (2) with $k_{det} = 0$). The ability of these two model descriptions to describe colloid attachment in the batch systems will be discussed below.

As it was mentioned earlier, to further examine the reversibility of attachment, and to determine the correct model formation to describe the batch experiments, after completion of the attachment phase shown in Fig. 1, the colloid suspension in the batch tubes was removed and replaced with colloid-free electrolyte solution of the same chemical composition. The tubes were subsequently shaken for another 2 h, and the aqueous colloid concentration was measured. The colloid concentration was found to be negligible (data not shown), demonstrating that the detachment rate was very slow. Moreover, the attachment/detachment model predicts that batch results will be independent of the initial colloid concentration (C_0) assuming a linear equilibrium isotherm, whereas the attachment/blocking model predicts a strong sensitivity to C_0. As it was mentioned earlier, additional batch experiments were conducted using different C_0 values for 0.5 and 0.1 μm colloids in 50 mM solution. Fig. 2 presents plots of C/C_0 as a function of time when different C_0 values were used. It is observed that the batch results were found to be highly sensitive to C_0. However, it was found out that the fitted values of k_{att} and S_{max} determined from the experiments with the lower C_0 (i.e. 9.1×10^7, and 2.8×10^{10} N_c mL^{-1} for the 0.5, and 0.1 μm colloids, respectively) simulated the observed colloid concentrations of the other experiments with higher C_0 (see Fig. 2). Consequently, results from the above experiments were consistent with the attachment/blocking model, but not with the attachment/detachment model. Similarly, Jin et al. (1997) demonstrated that attachment sites for viruses were limited and interpreted their batch results using an irreversible attachment process. Therefore, the attachment/blocking model was used to describe the batch data shown in Fig. 1 and the simulation results are shown in this figure.

Table 2 provides a summary of fitted values of k_{att} and S_{max} determined through inverse modeling and also calculated values of S_f (Eq. (6)). The irreversible attachment and blocking model provided an excellent description of the batch data ($R^2 > 0.95$). Inspection of Table 2 reveals that higher values of k_{att} and S_{max} occurred when the IS was increased and the colloid size was decreased. Higher values of k_{att} and S_{max} with high IS are expected because of compression of the double layer thickness that produces a lower energy barrier and greater depth in the secondary minima (Table 1), and an increase in the influence of nanoscale heterogeneities (Bradford and Torkzaban, 2012; Duffadar and Davis, 2008). Smaller colloids are more susceptible to the influence of nanoscale heterogeneities (Bradford and Torkzaban, 2013; Bradford et al., 2013; Darbha et al., 2010), and the diffusion coefficient is also larger. Both of these factors will produce larger values of k_{att} for smaller colloids, whereas the influence of nanoscale heterogeneities will contribute to larger values of S_{max}.

Table 2 indicates that calculated values of S_f were very small (<2%), especially for larger colloid sizes. The entire collector surface is expected to contribute to colloid attachment ($S_f = 100\%$) under fully favorable attachment conditions. However, these S_f values suggest that highly unfavorable attachment conditions prevailed, even when the IS was very high and standard DLVO calculations predicted favorable attachment conditions (Table 1). This information suggests that other factors were contributing to the reduction in colloid attachment in the batch systems.

Numerous deviations from standard DLVO predictions have been reported, especially in the presence of net repulsive electrostatic interactions (Bhattacharjee et al., 1998; Duffadar and Davis, 2007, 2008; Ma et al., 2011; Shen et al., 2010, 2012; Suresh and Walz, 1996). DLVO theory assumes that the colloid and collector surfaces are geometrically smooth (Hoek and Agarwal, 2006; Shen et al., 2012). Conversely, natural solid surfaces and colloids always exhibit some degree of surface roughness (Morales et al., 2009; Shellenberger and Logan, 2002; Suresh and Walz, 1996). For example, Fig. 3 presents SEM images of our quartz sand that demonstrate various degrees of surface roughness (number and size). DLVO theory has been extended to incorporate the influence of nanoscale roughness on interaction energies (Bradford and Torkzaban, 2013; Hoek and Agarwal, 2006; Shen et al., 2012). Results indicate that colloid interactions are strongly dependent on surface roughness properties (e.g., height, cross-sectional area,

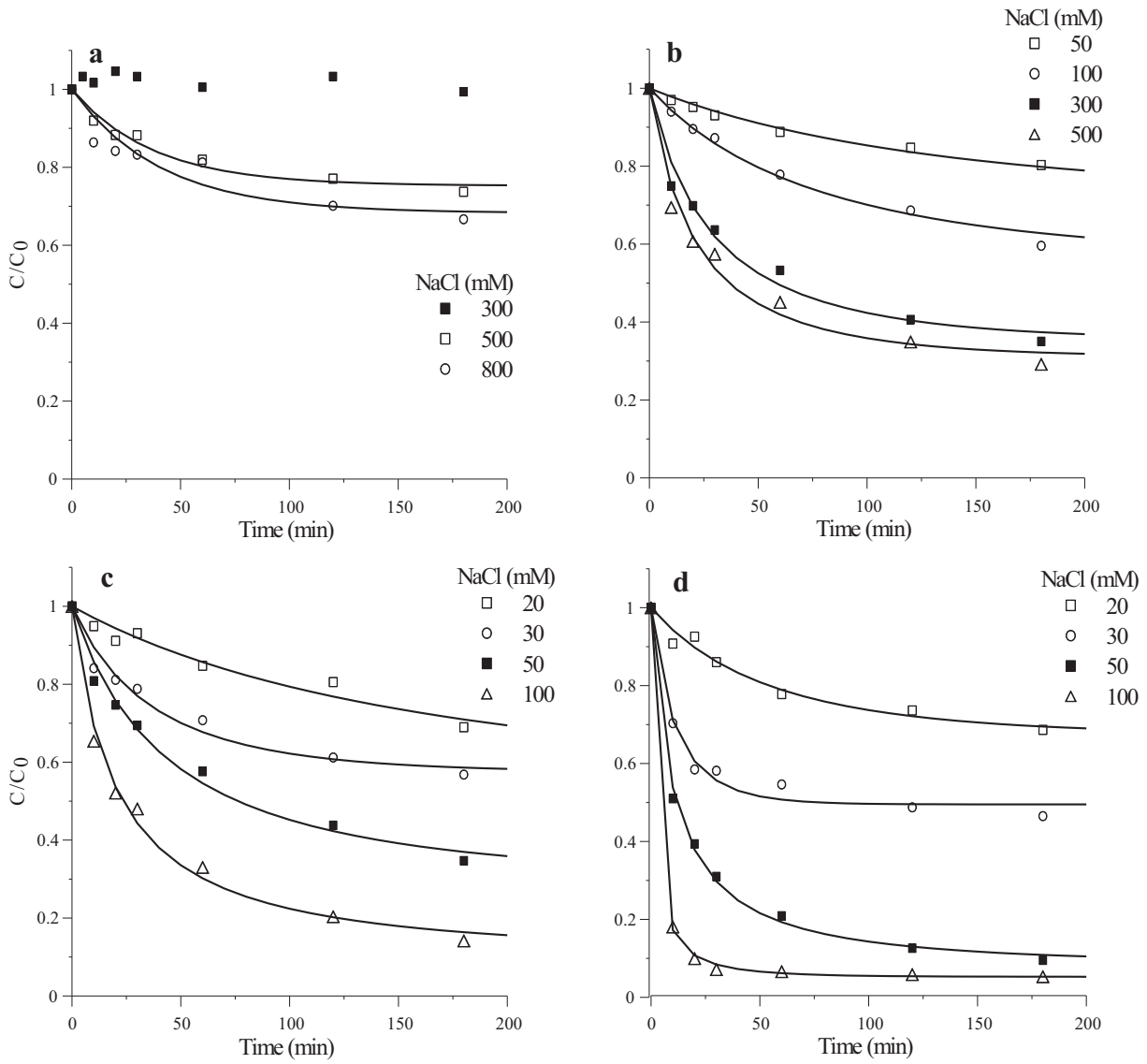

Fig. 1. Plots of observed (symbols) and simulated (lines) colloid concentrations in the batch experiments for various IS of (a) 2 μm, (b) 1 μm, (c) 0.5 μm and (d) 0.1 μm colloids. Simulations considered an irreversible attachment with a blocking behavior. Table 2 provides the fitted values of k_{att} and S_{max}.

and number), as well as the colloid size and solution IS. The magnitudes of the energy barrier and depth of the secondary minima are reduced on rough surfaces in comparison with smooth surfaces (Bradford and Torkzaban, 2013; Shen et al., 2012). This decrease in interaction energy on rough surfaces has been attributed to increased van der Waals attraction at smaller separation distances and increased electrostatic repulsion at larger separation distances (Bradford and Torkzaban, 2013). Primary minimum interactions are therefore expected to increase on surfaces with nanoscale roughness, whereas secondary minimum interactions will decrease.

DLVO theory predicts an infinite depth of the primary minimum and therefore irreversible attachment on smooth surfaces. Conversely, the depth of primary minimum is finite on rough surfaces, and can even be eliminated when Born repulsion is considered (Bradford and Torkzaban, 2013; Shen et al., 2012). A weak primary minimum interaction on rough surfaces will be susceptible to removal by hydrodynamic forces (Bergendahl and Grasso, 2000; Shen et al., 2012). The hydrodynamic force that acts on colloids near collector surfaces increases with the cube of the colloid radius (Bergendahl and Grasso, 1999; Bradford et al., 2011; Shen et al., 2010; Torkzaban et al., 2007). Consequently, low values of S_f (<2%) in our batch systems, especially for larger colloids, are consistent with weak secondary (IS ≤ 50 mM) and primary (IS ≥ 100 mM) minimum interactions on rough surfaces that could have been overcome by hydrodynamic forces.

The SEM images of sand grains in the batch experiments shown in Fig. 3 further reveal colloid attachment in depression regions where drag forces are negligible. If colloids can access

Table 2
Experimental conditions and fitted model parameters for column and batch experiments.

	IS (mM)	Size (μm)	k_{att} (min^{-1})	S_{max}/C_0 cm^3/g	S_{max} (No/g)	S_f (%)
Batch	20	0.1	0.01	0.32	9.1×10^9	0.67
	30	0.1	0.05	0.50	1.4×10^{10}	1.06
	50	0.1	0.09	0.91	2.6×10^{10}	1.92
	100	0.1	0.56	0.95	2.7×10^{10}	1.99
	20	0.5	0.00	0.46	4.2×10^7	0.08
	30	0.5	0.01	0.42	3.9×10^7	0.07
	50	0.5	0.02	0.70	6.4×10^7	0.12
	100	0.5	0.05	0.89	8.1×10^7	0.15
	300	0.5	0.32	0.94	8.5×10^7	0.16
	30	1	0.00	0.28	3.2×10^6	0.02
	50	1	0.01	0.44	5.0×10^6	0.04
	100	1	0.03	0.65	7.4×10^6	0.06
	300	1	0.04	0.69	7.9×10^6	0.06
	500	2	0.01	0.25	3.6×10^5	0.01
	800	2	0.07	0.31	4.4×10^5	0.01
Column	10	0.1	0.01	0.20	4.5×10^9	0.33
	30	0.1	0.14	0.82	1.9×10^{10}	1.39
	50	0.1	0.35	0.81	1.9×10^{10}	1.37
	5	0.5	0.04	2.66	1.6×10^8	0.30
	10	0.5	0.07	5.00	3.1×10^8	0.57
	50	0.5	0.13	ND[a]	ND	ND
	5	2	0.04	ND	ND	ND
	10	2	0.09	ND	ND	ND
	50	2	0.12	ND	ND	ND

[a] Not determined.

these low velocity regions, then these locations will be hydrodynamically favorable for colloid retention. Indeed, S_f values increased in the order of 2, 1, 0.5 and 0.1 μm colloids. This observation suggests that the greater attachment of smaller colloids (0.5 and 0.1 μm) primarily occurred on rough locations composed of ridges and valleys because of negligible hydrodynamic forces associated with these regions.

3.3. Column experiments

Fig. 4 presents observed and simulated BTCs for 2 (Fig. 4a), 0.5 (Fig. 4b), and 0.1 μm (Fig. 4c) colloids in the various IS solutions. Here normalized effluent concentrations (C/C_0) are plotted against the number of pore volumes. The simulations were obtained from the solution of Eqs. (4) and (5) using fitted values of k_{att}, S_{max} and λ. The value of k_{det} in these simulations was set to zero because we observed negligible tailing in the BTCs. The dispersivity coefficient (λ) was estimated by fitting the solution of Eq. (4) to the conservative tracer ($NaNO_3$) breakthrough data (data not shown). This value of λ was low (0.04 cm) as expected for an 11 cm column. The overall agreement between modeled and measured BTCs was excellent, with R^2 values ranging from 0.96 to 0.99.

Table 2 summarizes experimental conditions, fitted values of k_{att} and S_{max}, and calculated values of S_f (Eq. (6)) for the column experiments. It should be mentioned that the slope of the rising limb of the BTC was sometimes negligible (e.g., 2 μm), and in this cases a unique determination of S_{max} was not possible.

Very little colloid retention occurred when deionized water (IS ~ 0) was used as the background solution. Conversely, the amount of colloid retention and corresponding values of k_{att} and S_{max}, increased with IS. For example, more than 95% of the injected colloids (2, 0.5, and 0.1 μm) were retained in the sand when the IS was 50 mM. An increase in colloid retention with IS occurs because of compression of the double layer thickness that produces a lower energy barrier and greater depths in the primary and secondary minima, and an increase in the influence of nanoscale heterogeneities (Bradford and Torkzaban, 2012; Duffadar and Davis, 2008). The BTCs also exhibited blocking behavior (a decreasing rate of retention) as available retention sites were filled. This trend can be seen in BTCs for 0.1 μm colloids when IS ≥ 10 mM, as well as to a lesser extent for 0.5 μm

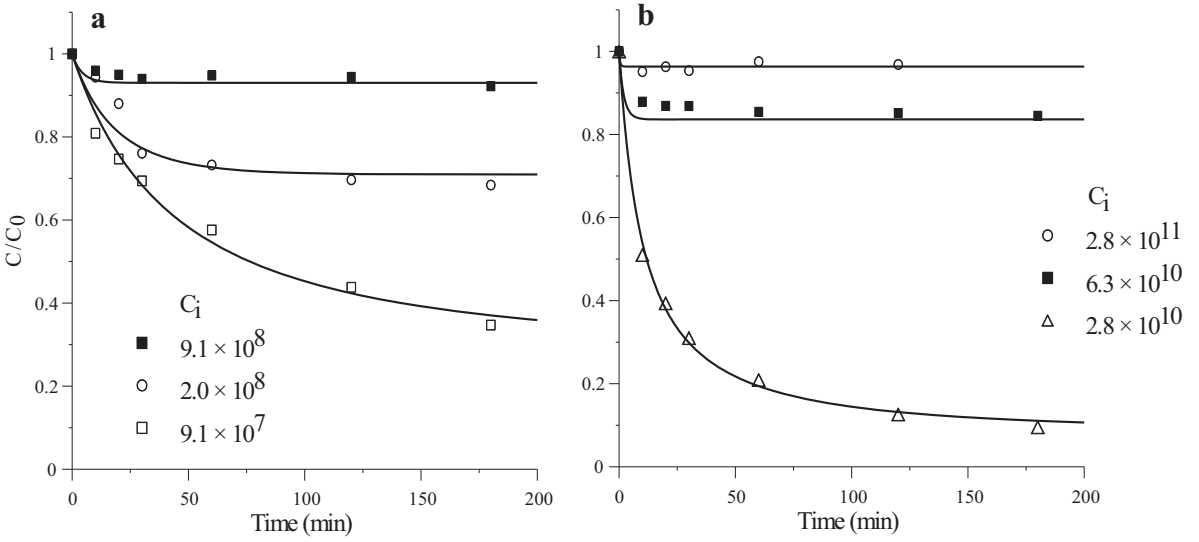

Fig. 2. Plots of observed (symbols) and simulated (lines) colloid concentrations in the batch attachments at 50 mM of (a) 0.5 μm and (b) 0.1 μm colloids when different initial colloid concentrations were used. Simulations considered an irreversible attachment with a blocking behavior.

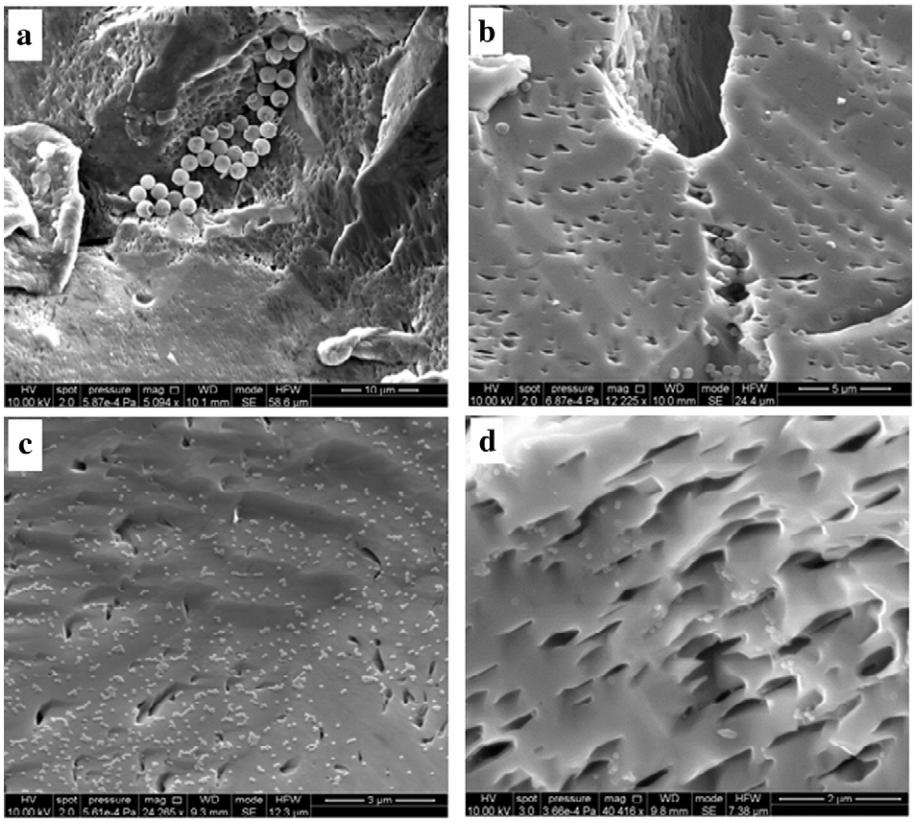

Fig. 3. Representative SEM images of colloids attached on sand grains in the batch experiments (a) 2 μm colloid at IS of 800 mM, (b) 0.5 μm colloid at IS of 300 mM, and (c & d) 0.1 μm colloid at IS of 100 mM.

colloids when the IS = 5 and 10 mM. Blocking also produces a delay in the arrival of the BTCs for 0.1 μm colloids when the IS ≥ 10 mM because of the high value of k_{att} for these smaller colloids (Torkzaban et al., 2010b, 2012). A linear, equilibrium retardation model cannot describe this delay, because detachment was not observed in the tailing of the BTCs.

3.4. Comparison of batch and column results

The detachment rates were found to be very slow in both batch and column experiments. The amount of colloid retention, k_{att}, and S_f were higher in column than batch experiments (Table 2), especially for larger colloids. Discrepancies between batch and column studies have been found by others (Jin et al., 1997; Powelson and Gerba, 1994; Torkzaban et al., 2008). The greater colloid retention, k_{att}, and S_f in column compared to batch studies cannot be attributed to stronger adhesive forces because the batch experiments were conducted over a much wider range of IS that should have provided even stronger adhesive forces (Table 2). Our batch results (especially with 2 and 1 μm colloids) clearly demonstrate that the adhesive interaction energy between the colloids and sand surfaces was not strong enough to produce colloid attachment, even at an IS that was as high as 500 or 800 mM. Furthermore, rates of colloid mass transfer from the aqueous to the solid phase are expected to be greater for continuously mixed batch than those of column studies (Sadeghi et al., 2013). Consequently, it is logical to anticipate that differences in the amount of colloid retention, values of k_{att} and S_f in column and batch studies reflect the influence of hydrodynamics, pore structure, and sand surface morphology (to be discussed below).

Previous column studies have shown that majority retained colloids can be released and recovered when the sand was excavated and suspended in electrolyte solutions of the same IS as used in the transport experiment (Bradford et al., 2009; Li et al., 2004; Tong et al., 2005; Torkzaban et al., 2008). We also observed that retained 2 μm colloids in IS = 50 mM solution were completely recovered from the column after the sand was excavated and the pore structure was eliminated (data not shown). This finding is consistent with the results of our batch experiments (Fig. 1) and demonstrated that the 2 μm colloids were weakly attached onto the quartz sand surface. Colloid retention is well-known to depend on both the solution and solid phase chemical conditions (Ryan and Elimelech, 1996) and the system hydrodynamics (Duffadar and Davis, 2007; Torkzaban et al., 2007). Rolling has been demonstrated to be the dominant mechanism of colloid detachment from solid surfaces under laminar flow conditions (Duffadar and Davis, 2008; Torkzaban et al., 2007). A balance of applied hydrodynamic (T_H) and resisting adhesive (T_A) torques therefore determines conditions for colloid immobilization and rolling (Bradford et al., 2011). Colloid immobilization occurs when $T_H \leq T_A$, whereas rolling occurs when $T_H > T_A$. It should be noted that some researchers have neglected the effect of T_A altogether and implicitly assumed that colloid immobilization only occurs in an infinite primary minimum (Johnson et al.,

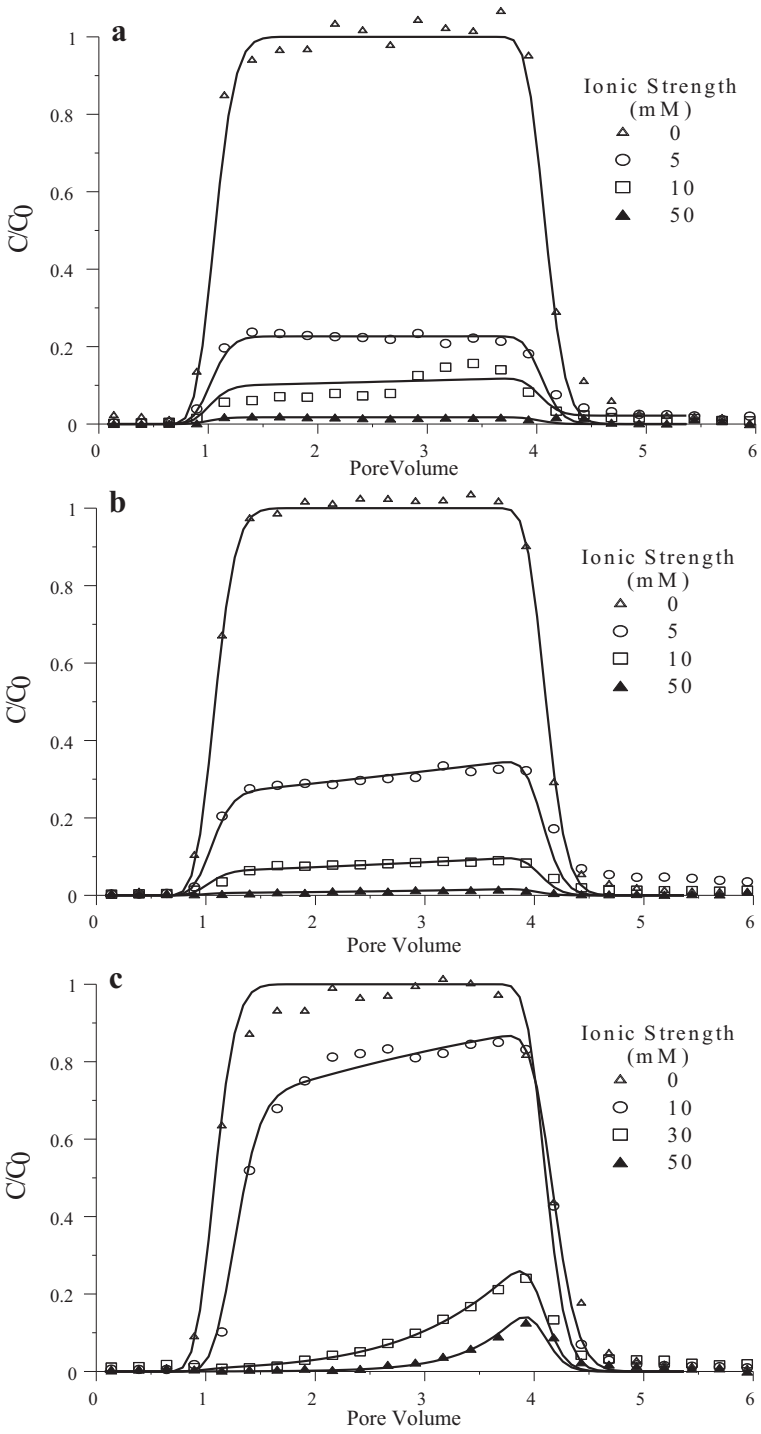

Fig. 4. Plots of observed (symbols) and simulated (lines) column breakthrough concentrations for various IS of (a) 2 μm, (b) 0.5 μm and (c) 0.1 μm colloids. Simulations considered attachment and blocking. Table 2 provides information about predicted k_{att} and S_{max}.

2007; Yang et al., 1998). However, this approach does not allow for colloid immobilization due to a secondary energy minimum in the presence of fluid flow (Torkzaban et al., 2008). Furthermore, this paradigm is not consistent with our batch results demonstrating a limited colloid attachment ($S_f < 2\%$) under unfavorable attachment conditions.

The sand surface morphology, which consists of large number of depressions, protrusions, nano- to micro-scale roughness, is known to influence the values of T_H and T_A because of their influence on the lever arms (Bradford et al., 2013; Shen et al., 2010). In particular, roughness will decrease the lever arm for T_H, and dramatically increase the lever arm for

T_A. When the roughness height is greater than the colloid radius (r_c) the lever arms for T_H and T_A equal 0 and r_c, respectively. Grain–grain contacts will similarly influence the values of T_H and T_A. Consequently, greater amounts of colloid immobilization occur on microscopically rough than on smooth surfaces, and at grain–grain contact points. Bradford et al. (2013) conducted a balance of T_H and T_A over a porous medium surface that contained random roughness of a given height to determine the value of S_f under unfavorable attachment conditions. The S_f values depended on the solution IS, r_c, roughness height and fraction, and Darcy velocity (q_w). Colloid immobilization was demonstrated to occur on a rough surface in the absence of attachment, and may therefore be considered as a surface straining process.

The direction and magnitude of T_H and T_A are relatively constant with time at a particular location on the sand surface in a steady-state column experiment. Consequently, colloid retention on the collector surface may occur at locations where $T_H \leq T_A$. Conversely, the direction and magnitude of T_H and T_A will dramatically change with time at a particular location in continuously mixed batch systems. Conditions for colloid immobilization in the batch system will therefore constantly change with the direction of the hydrodynamic forces, even if the magnitude of the hydrodynamic force is small. The overall value of S_f and the amount of colloid retention is therefore expected to be much smaller in a batch than that of a column system. These observations suggest that it is not possible to adopt a protocol (like the solid/water ratio, speed and direction of shaking) to obtain comparable results between batch and column systems. Consistent with other studies (Bales et al., 1991; Sadeghi et al., 2013; Schijven et al., 2000; Zhao et al., 2008), it appears that saturated column experiments provides a better approach for studying colloid (e.g. viruses, bacteria, engineered nanoparticles) transport and retention than batch techniques.

4. Conclusions

The bulk of existing colloid literature considers colloid deposition in porous media to be primarily controlled by interaction energies of colloids with grain surfaces. If this was the controlling mechanism, then batch results would have been reliable and comparable with those of column experiments. However, once a colloid collides with the SWI, attachment depends on a combination of forces and torques that act on the colloid at this location. These forces and torques include hydrodynamic drag and lift, electrical double-layer repulsion (or attraction), London–van der Waals interaction, and applied hydrodynamic and resisting adhesive torques. Of particular interest is the lever arm incorporated in the hydrodynamic and adhesive torques which depends on size and fraction of surface roughness. Colloid retention in flow systems (e.g. column) and to some extent in batch system for small colloids likely occurs in the regions on the grain surfaces where the roughness provides a favorable location for retention due to lever arm considerations. These locations on grain surfaces provide optimum locations for colloids that are likely associated with the solid phase either via secondary energy minimum or shallow primary minimum, to be retained due to reduced hydrodynamic forces and enhanced adhesive torque.

Our results indicate that in the presence of an energy barrier (unfavorable attachment conditions), the deposition behavior of colloids in batch system is inconsistent with those of column experiments. Specifically, the fraction of surface area available for attachment is significantly lower than that of column experiments. Deviation between batch and column results is increasingly significant for larger colloids. Predictions based on classical DLVO theory were found to inadequately describe interaction energies between colloids and natural surfaces which are always rough ranging from nano- to micro- scale. This implies that surface roughness plays an important role in determining the interaction energies and torque balances between the colloids and collector surfaces. Indeed, it is expected that the surface roughness will be more important, if not overriding, than chemical heterogeneities. Based on information shown in this study, it is clear that the hydrodynamic forces and surface roughness are the dominant factors controlling colloid deposition in batch and column experiments.

Acknowledgment

This work was supported by the Gas Industry Social and Environmental Research Alliance (GISERA). GISERA is a collaborative vehicle established by CSIRO and Australia Pacific LNG to undertake publicly reported research addressing the socio-economic and environmental impacts of Australia's natural gas industries. For more details about GISERA visit www.gisera.org.au. We would like to thank Mike Donn from CSIRO Land and Water for his comment that helped to strengthen the article.

References

Adamczyk, Z., Siwek, B., Zembala, M., Belouschek, P., 1994. Kinetics of localized adsorption of colloid particles. Adv. Colloid Interf. Sci. 48, 151–280.

Bales, R.C., Hinkle, S.R., Kroeger, T.W., Stocking, K., Gerba, C.P., 1991. Bacteriophage adsorption during transport through porous-media — chemical perturbations and reversibility. Environ. Sci. Technol. 25 (12), 2088–2095.

Bergendahl, J., Grasso, D., 1999. Prediction of colloid detachment in a model porous media: thermodynamics. AlChE J. 45 (3), 475–484.

Bergendahl, J., Grasso, D., 2000. Prediction of colloid detachment in a model porous media: hydrodynamics. Chem. Eng. Sci. 55 (9), 1523–1532.

Bhattacharjee, S., Ko, C.H., Elimelech, M., 1998. DLVO interaction between rough surfaces. Langmuir 14 (12), 3365–3375.

Bradford, S.A., Kim, H.N., Haznedaroglu, B.Z., Torkzaban, S., Walker, S.L., 2009. Coupled factors influencing concentration-dependent colloid transport and retention in saturated porous media. Environ. Sci. Technol. 43 (18), 6996–7002.

Bradford, S.A., Torkzaban, S., 2012. Colloid adhesive parameters for chemically heterogeneous porous media. Langmuir 28 (38), 13643–13651.

Bradford, S.A., Torkzaban, S., 2013. Colloid interaction energies for physically and chemically heterogeneous porous media. Langmuir 29 (11), 3668–3676.

Bradford, S.A., Torkzaban, S., Wiegmann, A., 2011. Pore-scale simulations to determine the applied hydrodynamic torque and colloid immobilization. Vadose Zone J. 10 (1), 252–261.

Bradford, S.A., Torkzaban, S., Kim, H., Simunek, J., 2012. Modeling colloid and microorganism transport and release with transients in solution ionic strength. Water Resour. Res. 48 (9).

Bradford, S.A., Torkzaban, S., Shapiro, A., 2013. A theoretical analysis of colloid attachment and straining in chemically heterogeneous porous media. Langmuir 29 (23), 6944–6952.

Bradford, S.A., Wang, Y., Kim, H., Torkzaban, S., Šimůnek, J., 2014. Modeling microorganism transport and survival in the subsurface. J. Environ. Qual. 43 (2), 421–440.

Brown, D.G., Abramson, A., 2006. Collision efficiency distribution of a bacterial suspension flowing through porous media and implications for field-scale transport. Water Res. 40 (8), 1591–1598.
Chrysikopoulos, C.V., Aravantinou, A.F., 2012. Virus inactivation in the presence of quartz sand under static and dynamic batch conditions at different temperatures. J. Hazard. Mater. 233, 148–157.
Darbha, G.K., Schaefer, T., Heberling, F., Luettge, A., Fischer, C., 2010. Retention of latex colloids on calcite as a function of surface roughness and topography. Langmuir 26 (7), 4743–4752.
Derjaguin, B., Landau, L., 1941. Theory of the stability of strongly charged lyophobic sols and of the adhesion of strongly charged particles in solutions of electrolytes. Acta Phys. Chim U.R.S.S. 14, 633–662.
Duffadar, R.D., Davis, J.M., 2007. Interaction of micrometer-scale particles with nanotextured surfaces in shear flow. J. Colloid Interface Sci. 308 (1), 20–29.
Duffadar, R.D., Davis, J.M., 2008. Dynamic adhesion behavior of micrometer-scale particles flowing over patchy surfaces with nanoscale electrostatic heterogeneity. J. Colloid Interface Sci. 326 (1), 18–27.
Ginn, T.R., Wood, B.D., Nelson, K.E., Scheibe, T.D., Murphy, E.M., Clement, T.P., 2002. Processes in microbial transport in the natural subsurface. Adv. Water Resour. 25 (8–12), 1017–1042.
Gregory, J., 1981. Approximate expressions for retarded Van der Waals interaction. J. Colloid Interface Sci. 83 (1), 138–145.
Harvey, R.W., Garabedian, S.P., 1991. Use of Colloid Filtration Theory in Modeling Movement of Bacteria through a Contaminated Sandy Aquifer. Environ. Sci. Technol. 25 (1), 178–185.
Harvey, R.W., Harms, H., Landkammer, L., 2002. Transport of microorganism in the terrestrial subsurface: in situ and laboratory methods. Manual of Environmental Microbiology.
Hoek, E.M.V., Agarwal, G.K., 2006. Extended DLVO interactions between spherical particles and rough surfaces. J. Colloid Interface Sci. 298 (1), 50–58.
Hogg, R., Healy, T.W., Dw, Fuersten, 1966. Mutual coagulation of colloidal dispersions. Trans. Faraday Soc. 62 (522P), 1638–1651.
Jin, Y., Flury, M., 2002. Fate and transport of viruses in porous media. Adv. Agron. 77, 39–102.
Jin, Y., Yates, M.V., Thompson, S.S., Jury, W.A., 1997. Sorption of viruses during flow through saturated sand columns. Environ. Sci. Technol. 31 (2), 548–555.
Johnson, P.R., Elimelech, M., 1995. Dynamics of colloid deposition in porous-media — blocking based on random sequential adsorption. Langmuir 11 (3), 801–812.
Johnson, W.P., Li, X., Assemi, S., 2007. Deposition and re-entrainment dynamics of microbes and non-biological colloids during non-perturbed transport in porous media in the presence of an energy barrier to deposition. Adv. Water Resour. 30 (6–7), 1432–1454.
Kim, H.N., Bradford, S.A., Walker, S.L., 2009. *Escherichia coli* O157:H7 transport in saturated porous media: role of solution chemistry and surface macromolecules. Environ. Sci. Technol. 43 (12), 4340–4347.
Lazouskaya, V., Jin, Y., 2008. Colloid retention at air–water interface in a capillary channel. Colloids Surf. A Physicochem. Eng. Asp. 325 (3), 141–151.
Li, X.Q., Johnson, W.P., 2005. Nonmonotonic variations in deposition rate coefficients of microspheres in porous media under unfavorable deposition conditions. Environ. Sci. Technol. 39 (6), 1658–1665.
Li, X.Q., Scheibe, T.D., Johnson, W.P., 2004. Apparent decreases in colloid deposition rate coefficients with distance of transport under unfavorable deposition conditions: a general phenomenon. Environ. Sci. Technol. 38 (21), 5616–5625.
Ma, H., Pazmino, E., Johnson, W.P., 2011. Surface heterogeneity on hemispheres-in-cell model yields all experimentally-observed non-straining colloid retention mechanisms in porous media in the presence of energy barriers. Langmuir 27 (24), 14982–14994.
Marquardt, D.W., 1963. An algorithm for least-squares estimation of nonlinear parameters. J. Soc. Ind. Appl. Math. 11 (2), 431–441.
Mondal, P.K., Sleep, B.E., 2013. Virus and virus-sized microsphere transport in a dolomite rock fracture. Water Resour. Res. 49 (2), 808–824.
Morales, V.L., Gao, B., Steenhuis, T.S., 2009. Grain surface-roughness effects on colloidal retention in the Vadose zone. Vadose Zone J. 8 (1), 11–20.
Pensini, E., Sleep, B.E., Yip, C.M., O'Carroll, D., 2012. Forces of interactions between bare and polymer-coated iron and silica: effect of ph, ionic strength, and humic acids. Environ. Sci. Technol. 46 (24), 13401–13408.
Powelson, D.K., Gerba, C.P., 1994. Virus removal from sewage effluents during saturated and unsaturated flow — through soil columns. Water Res. 28 (10), 2175–2181.
Ryan, J.N., Elimelech, M., 1996. Colloid mobilization and transport in groundwater. Colloids Surf. A Physicochem. Eng. Asp. 107, 1–56.
Sadeghi, G., Schijven, J.F., Behrends, T., Hassanizadeh, S.M., van Genuchten, M.T., 2013. Bacteriophage PRD1 batch experiments to study attachment, detachment and inactivation processes. J. Contam. Hydrol. 152, 12–17.
Schijven, J.F., Hassanizadeh, S.M., 2000. Removal of viruses by soil passage: overview of modeling, processes, and parameters. Crit. Rev. Environ. Sci. Technol. 30 (1), 49–127.
Schijven, J.F., Hassanizadeh, S.M., Dowd, S.E., Pillai, S.D., 2000. Modeling virus adsorption in batch and column experiments. Quant. Microbiol. 2 (1), 5–20.
Shellenberger, K., Logan, B.E., 2002. Effect of molecular scale roughness of glass beads on colloidal and bacterial deposition. Environ. Sci. Technol. 36 (2), 184–189.
Shen, C., Huang, Y., Li, B., Jin, Y., 2008. Effects of solution chemistry on straining of colloids in porous media under unfavorable conditions. Water Resour. Res. 44 (5).
Shen, C., Huang, Y., Li, B., Jin, Y., 2010. Predicting attachment efficiency of colloid deposition under unfavorable attachment conditions. Water Resour. Res. 46.
Shen, C., Li, B., Huang, Y., Jin, Y., 2007. Kinetics of coupled primary- and secondary-minimum deposition of colloids under unfavorable chemical conditions. Environ. Sci. Technol. 41 (20), 6976–6982.
Shen, C., Wang, L.-P., Li, B., Huang, Y., Jin, Y., 2012. Role of surface roughness in chemical detachment of colloids deposited at primary energy minima. Vadose Zone J. 11 (1).
Simoni, S.F., Harms, H., Bosma, T.N.P., Zehnder, A.J.B., 1998. Population heterogeneity affects transport of bacteria through sand columns at low flow rates. Environ. Sci. Technol. 32 (14), 2100–2105.
Simunek, J., van Genuchten, M.T., Sejna, M., 2005. The HYDRUS-1D software package for simulating the one-dimensional movement of water, heat, and multiple solutes in variably-saturated media — version 3.0, HYDRUS software series 1. Department of Environmental Sciences, University of California Riverside, Riverside, CA.
Suresh, L., Walz, J.Y., 1996. Effect of surface roughness on the interaction energy between a colloidal sphere and a flat plate. J. Colloid Interface Sci. 183 (1), 199–213.
Syngouna, V.I., Chrysikopoulos, C.V., 2010. Interaction between viruses and clays in static and dynamic batch systems. Environ. Sci. Technol. 44 (12), 4539–4544.
Thompson, S.S., Flury, M., Yates, M.V., Jury, W.A., 1998. Role of the air–water–solid interface in bacteriophage sorption experiments. Appl. Environ. Microbiol. 64 (1), 304–309.
Thompson, S.S., Yates, M.V., 1999. Bacteriophage inactivation at the air–water–solid interface in dynamic batch systems. Appl. Environ. Microbiol. 65 (3), 1186–1190.
Tong, M.P., Li, X.Q., Brow, C.N., Johnson, W.P., 2005. Detachment-influenced transport of an adhesion-deficient bacterial strain within water-reactive porous media. Environ. Sci. Technol. 39 (8), 2500–2508.
Torkzaban, S., Bradford, S.A., van Genuchten, M.T., Walker, S.L., 2008. Colloid transport in unsaturated porous media: the role of water content and ionic strength on particle straining. J. Contam. Hydrol. 96 (1–4), 113–127.
Torkzaban, S., Bradford, S.A., Walker, S.L., 2007. Resolving the coupled effects of hydrodynamics and DLVO forces on colloid attachment in porous media. Langmuir 23 (19), 9652–9660.
Torkzaban, S., Bradford, S.A., Wan, J., Tokunaga, T., Masoudih, A., 2013. Release of quantum dot nanoparticles in porous media: role of cation exchange and aging time. Environ. Sci. Technol. 47 (20), 11528–11536.
Torkzaban, S., Kim, H.N., Simunek, J., Bradford, S.A., 2010a. Hysteresis of colloid retention and release in saturated porous media during transients in solution chemistry. Environ. Sci. Technol. 44 (5), 1662–1669.
Torkzaban, S., Kim, Y., Mulvihill, M., Wan, J., Tokunaga, T.K., 2010b. Transport and deposition of functionalized CdTe nanoparticles in saturated porous media. J. Contam. Hydrol. 118 (3), 208–217.
Torkzaban, S., Wan, J., Tokunaga, T.K., Bradford, S.A., 2012. Impacts of bridging complexation on the transport of surface-modified nanoparticles in saturated sand. J. Contam. Hydrol. 136, 86–95.
Tufenkji, N., Elimelech, M., 2004. Correlation equation for predicting single-collector efficiency in physicochemical filtration in saturated porous media. Environ. Sci. Technol. 38 (2), 529–536.
Yang, C., Dabros, T., Li, D.Q., Czarnecki, J., Masliyah, J.H., 1998. Kinetics of particle transport to a solid surface from an impinging jet under surface and external force fields. J. Colloid Interface Sci. 208 (1), 226–240.
Yates, M.V., Yates, S.R., Wagner, J., Gerba, C.P., 1987. Modeling virus survival and transport in the subsurface. J. Contam. Hydrol. 1 (3), 329–345.
Zhao, B., Zhang, H., Zhang, J., Jin, Y., 2008. Virus adsorption and inactivation in soil as influenced by autochthonous microorganisms and water content. Soil Biol. Biochem. 40 (3), 649–659.